Preparation and Properties of Silica-Coated Cobalt Nanoparticles†

Yoshio Kobayashi,*,‡ Mitsuru Horie,‡ Mikio Konno,‡ Benito Rodríguez-González,§ and Luis M. Liz-Marzán*,§

Department of Chemical Engineering, Graduate School of Engineering, Tohoku University, Sendai 980-8579, Japan, and Departamento de Química Física, Universidade de Vigo, E-36200, Vigo, Spain

Received: December 18, 2002; In Final Form: January 20, 2003

The synthesis of monodispersed, amorphous cobalt nanoparticles coated with silica in aqueous/ethanolic solution is described. Both the core size and the silica shell thickness can be controlled through the synthetic conditions. Furthermore, the transformation of the cobalt cores into crystalline, metallic cobalt upon annealing in air is demonstrated through X-ray diffraction data. Both the initial, amorphous nanoparticles and their crystalline counterpart are magnetic, which promises important applications for ferrofluid preparation and for magnetic recording media.

1. Introduction

The extensive research carried out on the synthesis and characterization of magnetic nanoparticles, both in dispersion (ferrofluids)[1] and within nanostructures[2] are fully justified due to a whole range of applications that such systems can find in various fields such as magnetic inks,[3] isolating systems,[4] model systems for interparticle interactions,[5] or recording media.[6] In any of these studies and applications, it is of primary importance to control the surface properties of the nanoparticles. In the case of ferrofluids, the surface will be the main factor determining colloidal stability, and several pathways have been followed to enhance stability, from the use of specific surfactants[7−9] to the control of surface charge.[10] For the assembly of magnetic nanoparticles within nanostructures, a high degree of control on the interactions between neighboring nanoparticles is highly desirable to tailor the magnetic properties of the whole structure.

Some of the most representative magnetic materials are metal oxides such as various ferrites.[10−13] However, these are often obtained as mixtures of several oxides, which implies that the magnetic properties are not always well defined and reproducible. Apart from the magnetic metal oxides, pure metals such as, Fe, Co, and Ni and their metal alloys, are also used in various fields of magnetism.[14,15] The main difficulty for the use of pure metals arises from their instability toward oxidation in air, which becomes easier as the size gets smaller. Therefore, it is mandatory to develop methods to improve the chemical stability of the particles. One approach to chemical stabilization is the deposition of insulating shells on the nanoparticles surface that prevent the reaction of oxygen with the surface atoms. Noble metals have been deposited through reactions in microemulsions[16,17] or other chemical methods such as redox transmetalation.[18] Stable Ag@Co nanoparticles where Co is present in the shell were also recently reported.[19] Recently, Gedanken and co-workers reported a sonochemical procedure that leads to air-stable Co nanoparticles.[20] These authors claim that the stability arises from the formation of a carbon shell on the nanoparticle surface. However, the particles obtained are rather polydisperse and not very uniform.

The deposition of silica shells on magnetic particles has been used by several authors.[21−27] The advantages of silica are: exceptional stability of aqueous dispersions; easy surface modification that allows the preparation of nonaqueous colloids; easy control of interparticle interactions, both in solution and within structures, through shell thickness. Previous works involved the coating of hematite (Fe_2O_3) spindles,[21] which could be subsequently reduced to metallic iron in a dry state,[22] and much smaller magnetite (Fe_3O_4) clusters.[23−27] In such cases, coating was performed on an oxide, which easily binds to silica through OH surface groups. However, silica deposition on pure metal particles is more complicated because of the lack of OH groups on the metal surface. Therefore, it is necessary to use a primer to make the surface "vitreophilic".[28] This chemistry has been used for noble metals,[29,30] which are chemically very stable. An additional difficulty to be overcome in the case of cobalt is that it readily oxidizes in the presence of dissolved oxygen.

In this paper we describe a procedure that permits the preparation of Co nanoparticles of various sizes in aqueous solution and their coating with well-defined silica shells. The Co cores so obtained are amorphous, but can be crystallized by annealing in a standard oven in air, which demonstrates the protective effect of the silica coating against oxidation. A preliminary magnetization study shows that high saturation magnetization values (120−180 emu/g of Co) can be obtained for core−shell particles with crystalline cores, while keeping a soft magnetic behavior (coercive fields between 200 and 300 Oe).

2. Experimental Section

2.1. Materials. Cobalt chloride hexahydrate (Wako Pure Chem. Ind., 99.5%), sodium borohydride (Wako Pure Chem. Ind., 90%), citric acid monohydrate (Wako Pure Chem. Ind., 99.5%), 3-aminopropyl-trimethoxysilane (APS) (Aldrich, 97%), tetraethyl orthosilicate (TEOS) (Wako Pure Chem. Ind., 95%), and ethanol (Wako Pure Chem. Ind., 99.5%) were used as received. Deionized water (18 MΩ·cm) was used for all the preparations.

† Part of the special issue "Arnim Henglein Festschrift".

* To whom correspondence should be addressed. (Yoshio Kobayashi) E-mail: yoshio@mickey.che.tohoku.ac.jp. (Luis M. Liz-Marzán) E-mail: lmarzan@uvigo.es.

‡ Tohoku University.

§ Universidade de Vigo.

10.1021/jp027759c CCC: $25.00
Published on Web 02/28/2003

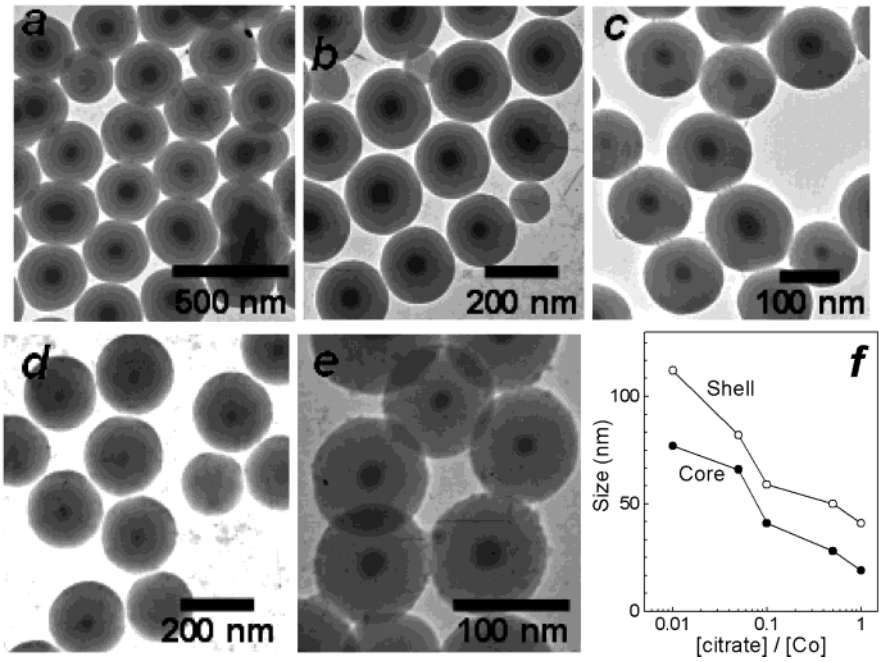

Figure 1. TEM images of $Co@SiO_2$ particles. [citrate]/[Co] = (a) 0.01, (b) 0.05, (c) 0.1, (d) 0.5, and (e) 1. (f) Average core diameter and shell thickness as a function of [citrate]/[Co] ratio.

2.2. Preparation. The preparation of cobalt particles was performed by addition of 0.2 mL of 0.4 M $CoCl_2$ in H_2O to 200 mL of 4×10^{-3} M $NaBH_4$ in a deaerated aqueous solution containing citric acid (4×10^{-6} (sample 1), 2×10^{-5} (sample 2), 4×10^{-5} (sample 3), 2×10^{-4} (sample 4), and 4×10^{-4} M (sample 5)), and particle formation was manifested by a gray coloration of the dispersion. Nitrogen bubbling was maintained during the reactions. Silica coating was performed by addition of an ethanolic solution containing APS and TEOS in a molar ratio 1:9 (typically 800 mL of ethanol containing 14.4 μL of APS and 169 μL of TEOS added onto 200 mL of the aqueous Co colloid), 1 min after mixing the $CoCl_2$ and $NaBH_4$ solutions. In the water/ethanol mixture, attachment of APS onto the surface of cobalt particles takes place, followed by hydrolysis/condensation of both APS and TEOS which results in the formation of the silica shells. For crystallization of silica-coated cobalt ($Co@SiO_2$), the $Co@SiO_2$ particles were separated from dispersion by centrifugation and drying, and the resulting powder was annealed in air at temperatures between 200 and 700 °C for 2 h.

2.3. Characterization. The samples were characterized by transmission electron microscopy (TEM), X-ray diffraction (XRD) and vibrating sample magnetometry (VSM). TEM was performed on a Zeiss LEO 912 OMEGA microscope operating at 100 kV of accelerating voltage and a Philips CM20 with an acceleration voltage of 200 kV. The samples for TEM were prepared by dropping and evaporating the obtained $Co@SiO_2$ colloid on top of a collodion-coated copper grid. XRD measurements were taken with a Rigaku RU-200A diffractometer at 40 kV and 30 mA with Cu Kα radiation. VSM measurements were performed for $Co@SiO_2$ powder in a Toei VSM-5-15 magnetometer.

3. Results and Discussion

3.1. Colloid Synthesis. The procedure and conditions described in the Experimental Section were found to be optimal for the production of stable colloids. In particular, when lower amounts of APS and TEOS were used, Co particles could not be observed in TEM. This means that the binding of APS to the particles and subsequent condensation were not sufficient to protect the cobalt core against both oxidation and aggregation.

The ratio between citrate and Co^{2+} ions was found to be an important parameter, since it determines the size of the Co cores within the final core−shell colloids. Typical TEM pictures of the particles prepared with different ratios (ranging from 0.01 to 1) is shown in Figure 1, where a high contrast is observed between the Co core and the SiO_2 shell. The presence of Co, Si and O was confirmed by energy-dispersive spectrometry (EDS) (not shown). It is interesting to note that no peaks for contaminant elements such as boron were observed with EDS (only additional peaks for Cu were present due to the TEM grid), which is probably due to the low molecular weight of this element, combined with a limited resolution of the instrument.

It is remarkable that, regardless of the citrate:Co molar ratio, a nearly perfect core−shell morphology is obtained, with rather monodisperse size distributions (both for the core and the shell) and very few particles with no core or more than one core. Such results demonstrate the high efficiency of this procedure, despite its simplicity, as compared to other nanoparticle silica-coating techniques previously reported.[24,29] The dependence of the core size on the relative amount of citrate present during the formation of the Co nanoparticles is related to the adsorption of citrate ions on the cobalt particle surface, preventing further growth through double layer repulsion between negatively charged cobalt particles. As shown in Figure 1f, the silica shell thickness also decreases with increasing citrate concentration, since the total surface area of the cobalt particles increased with decreasing core size.

Although the main concept behind the synthetic procedure basically coincides with that reported in refs 28−30, there are a few important differences which are worth mentioning. First, the surface priming and shell formation steps are performed simultaneously through the mixture of the Co nanoparticle aqueous dispersion and the solution of APS and TEOS in ethanol. This implies that the initial coating from sodium silicate

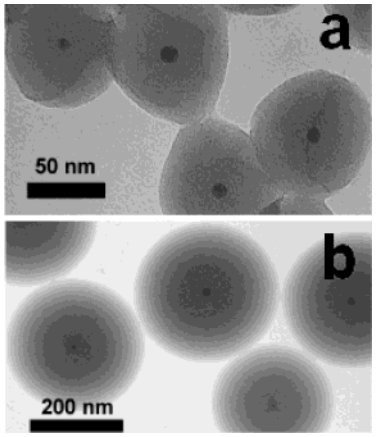

Figure 2. TEM images of $Co@SiO_2$ particles. (a) before and (b) after further growth of the silica shell.

used in refs 28−30 is not required here, thus simplifying the process. Second, the use of ammonia is not needed, which avoids complexation and oxidation reactions with the Co cores. Finally, in the present method the time at which the shell is deposited is crucial to control the stability of the final colloid, since the Co cores can aggregate and even oxidize if the timing is not correct.

Once the particles have been formed, the shell thickness can be grown further by addition of ammonia and TEOS.[31] One example is shown in Figure 2, for a core size of 15 nm. However, formation of thinner shells has not been possible because, as pointed out above, use of smaller amounts of APS and TEOS does not lead to stable colloids. Further optimization is needed toward this target.

3.2. Nanoparticle Crystallization. One of the main objectives of this work was the preparation of a system with interesting magnetic properties, which interactions could be controlled through the coating with a shell of nonmagnetic material. Thus, our interest was on the achievement of nanocrystalline cobalt cores surrounded by homogeneous silica shells. However, XRD shows that regardless of the molar ratio between citrate and Co, the as-prepared samples are amorphous, since the diffractograms are featureless. High-temperature annealing of the particles was considered as a means to drive the solid-state crystallization of the cores. Annealing at various temperatures up to 700 °C was performed for 2 h in a standard oven, and in the presence of air. Longer annealing processes lead to no improvement of crystallinity. The XRD results for samples 1−5 are shown in Figure 3. It can be observed that the temperature evolution of the diffractograms is not identical for all the samples studied. However, in all cases the material is amorphous at room temperature, but shows characteristic peaks for metallic Co upon heating at 400 or 500 °C, and crystalline silica (cristobalite) is formed at 700 °C, while the Co peaks disappear. The formation of metallic Co is an evidence of the protection that the silica shell exerts against oxidation of the core. Upon heating, this protection is more effective due to compression of the pores.[32] However, at higher temperatures, as silica crystallizes, cracks are likely to arise in the shell, thereby allowing diffusion of oxygen and oxidation of the core. Such a protection has previously been observed for CdS quantum dots, which undergo photodegradation in the presence of oxygen,[33] but remain unaltered upon silica coating.[34] This does not mean that the silica shell prevents any chemical reaction to take place at the cores,[30,35] but rather that surface sites prone to oxidation are blocked during coating. Upon annealing, the shell is likely to be compressed, which would provide almost full protection against external agents.

The sizes of the cobalt crystal domains were estimated from X-ray diffraction line broadening of the peak at 75.9° according

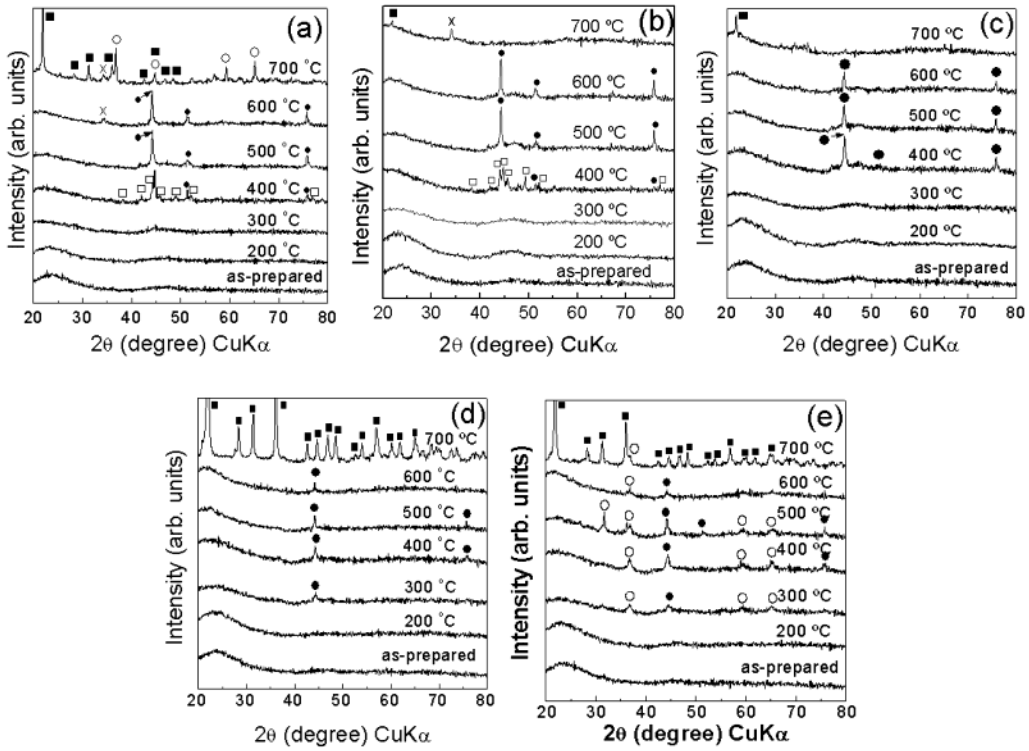

Figure 3. Evolution of XRD patterns of $Co@SiO_2$ nanoparticles upon annealing for 2 h in air at the temperatures indicated, for [citrate]:[Co] ratios as described in Figure 1. The symbols point to characteristic peaks of various compounds: (•) Co (cubic), Co_3O_4 (cubic), (■) SiO_2 (cristobalite), (□) Co_3B or Co_4B (orthorombic), and (×) CoO (cubic).

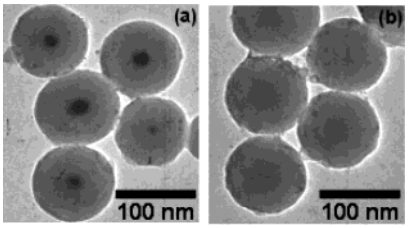

Figure 4. TEM micrographs of particles from sample 5 ([citrate]:[Co] = 1) after annealing at (a) 500 and (b) 600 °C.

to Scherrer equation, and values between 10 and 20 nm were obtained, regardless of core particle size and annealing temperature. This is an interesting result, since the core sizes range from 19 nm for sample 5 up to 77 nm for sample 1. This probably means that the larger cores are made of aggregates of smaller particles, which can easily be related to the insufficient amount of citrate ions during the synthesis.

In the remaining of this section, we discuss the differences encountered for the phases present for each sample at different temperatures.

In samples 1 and 2, several peaks attributed to cobalt boride such as Co_3B or Co_4B (orthorhombic) are observed at 400 °C, together with some peaks for metallic cobalt (cubic). However, at 500 and 600 °C, the peaks of cobalt boride disappear and the peaks of metallic cobalt become more intense. This seems to indicate that cobalt boride decomposes leading to the formation of borate and metallic cobalt. Upon annealing at 600 °C, a peak attributed to CoO (cubic) was also observed at 34.1°, which indicates partial oxidation of the cobalt cores. Annealing at 700 °C gives rise to a number of new peaks marked with solid squares, which were identified as cristobalite silica. Although pure silica gel is usually crystallized from amorphous state to the cristobalite phase by annealing above 1000 °C,[36] in the presence of sodium or borate ions the crystallization temperature can be lower because of the formation of a network structure around sodium or borate,[37] which are likely to be present from the starting chemicals. In sample 2 the cristobalite phase is not so evident at 700 °C, which may be related to a lower degree of impurities. This is also related to the lack of peaks due to Co_3O_4 (cubic) as compared to sample 1, since a lower crystallinity of the shell implies a lower chance of crack formation.

It is noteworthy that in samples 3−5 no peaks for cobalt borides were detected at any temperature, which may be related to a lower tendency to the formation of the borides for higher amounts of citrate. Also, while in samples 3 and 4 no cobalt oxides are observed, it seems that they coexist with metallic cobalt from 300 °C upward, which is probably related to the smaller particle size and related higher reactivity.

The disappearance of the peaks for metallic cobalt at high temperature can be related to the reaction of Co with Si. For some reason (the crystals may be too small or the compound amorphous), no peaks for related compounds have been observed, but TEM observation of the particles upon annealing reveals a clear change. As an example, TEM micrographs of particles from sample 5 that have been annealed in air at 500 and 600 °C are shown in Figure 4. It can be seen that, while upon annealing at 500 °C the core is still clearly differentiated from the shell, annealing at 600 °C leads to a loss of contrast and only a slightly darker area is visible about the center of the particle, which supports the idea of Co/Si compounds. At this higher temperature, the surface of the particles appears somewhat deformed, probably due to sintering. Similar experiments on other samples show disappearance of the cores at 700 °C, in agreement with the XRD data. It is also interesting to see that the core−shell morphology is intact after annealing, since this may be important for applications where nanostructures are made at room temperature and annealing is subsequently performed.

3.3. Magnetic Properties. Magnetic characterization of the particles was performed at room temperature for all the annealing temperatures reported in the previous section. As an example, Figure 5 shows the hysteresis loops for samples 2 and 4. The corresponding data for samples 1, 3, and 5 are provided as Supporting Information (Figures S1−S3). It should be stressed that these are raw data, where the magnetization is expressed in units of emu per gram of powder, which includes the diamagnetic shells.

In the figure it can be observed that magnetization can be saturated at relatively low applied magnetic fields for as-prepared samples as well as upon annealing at various temperatures. However, after annealing at 700 °C no magnetization is observed in the whole magnetic field range applied. In general, we can state that, as the particle size increases, the slope of the magnetization curve decreases, which indicates slow saturation, usually related to interactions between the magnetic dipoles present in the cobalt domains.[37] That behavior of slow saturation can be supported by our previous conclusion that the larger Co cores are formed by aggregates of smaller particles.

For the discussion of the magnetic properties and comparison of the different samples, we have summarized the data in two plots (saturation magnetization and coercive field vs annealing temperature), which are shown in Figure 6.

Figure 6a shows plots of the saturation magnetization as a function of annealing temperature for the different particle sizes obtained. In this plot, we recalculated the magnetization values

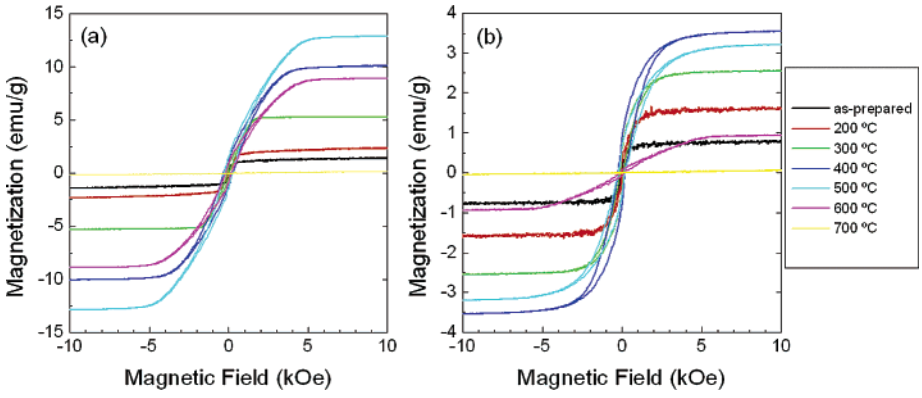

Figure 5. Hysteresis loops for samples (a) 2 and (b) 4 at the annealing temperatures indicated.

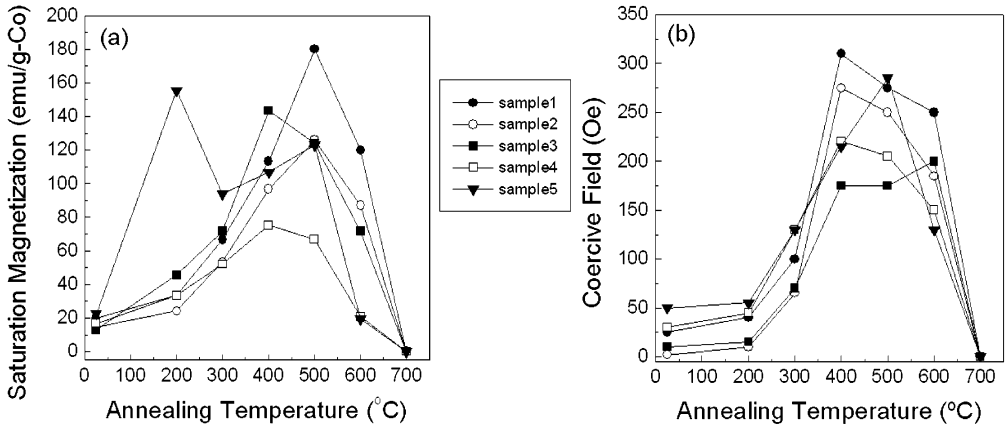

Figure 6. Room-temperature (a) saturation magnetization and (b) coercive field vs annealing temperature for samples 1−5.

to units of emu per gram of Co. For the calculation, we assumed that the core particles mainly contain cobalt, and derived the following equation:

$$W_{Co} = \frac{\rho_{Co}\, r_{core}^3}{\rho_{silica}\,(r^3 - r_{core}^3) + \rho_{Co}\, r_{core}^3} \qquad (1)$$

where the literature value of 8.9 g/mL[38] was used for the density of metallic cobalt, the density of amorphous silica, 1.87 g/mL, was measured by means of a specific gravity bottle for silica gel powder, and the radius of the core r_{core} and the coated sphere r were obtained by averaging TEM values (see Figure 1). With the exception of sample 5, the maximum values of saturation magnetization were obtained at 400 or 500 °C of annealing temperature. Those temperatures are in good agreement with the annealing temperatures at which the strongest XRD peaks of metallic cobalt were observed for each sample. However, for sample 5, the maximum saturation magnetization is found at 200 °C, while no remarkable XRD peak was observed at that annealing temperature. However, it should be taken into account that in this sample even at low annealing temperatures the presence of Co_3O_4 was detected by XRD, which means that eq 1 cannot be safely applied in this case.

The maximum saturation magnetizations obtained are comparable to those for bulk metallic cobalt (162 emu/g),[39] and for other metal and alloy nanoparticles.[20] It has been observed previously that as the surface/volume ratio increases (or the particle size decreases) the saturation magnetization decreases due to an increase in the disorder of the orientation of magnetic moments in the various sites,[40] which agrees with the results shown in Figure 6.

Figure 6b shows the dependence of the coercive field of $Co@SiO_2$ particles on the annealing temperature. For all samples, the coercive field increases with the annealing temperature up to 400−600 °C and then decreases down to zero. The annealing temperatures that gave a maximum coercive field (around 300 Oe) correspond again to those for the strongest XRD peak of metallic cobalt.

4. Conclusions

In summary, we have devised a simple chemical method for the synthesis and stabilization (both chemical and colloidal) of magnetic, amorphous Co nanoparticles surrounded by homogeneous shells of silica. The core−shell particles can be subsequently transformed in independent, crystalline nanoparticles upon annealing, which are stable in air for long periods of time. This novel type of composite magnetic nanoparticles has potential applications, both in the field of ferrofluids and in magnetic storage media. The controlled assembly of $Co@SiO_2$ nanoparticles is currently being studied and will be described in a subsequent report.

Acknowledgment. This work has been supported by the Spanish Xunta de Galicia (Project No. PGIDT01PXI30106PR), and Ministerio de Ciencia y Tecnología (Project No. BQU2001-3799). Y.K. acknowledges the Spanish Ministerio de Educación y Cultura for a personal grant. We express our thanks to Dr. Y. Ando and Dr. T. Miyazaki from the Department of Applied Physics, Graduate School of Engineering, Tohoku University, for assistance in the magnetic measurements and fruitful discussions.

Supporting Information Available: Figures S1−S3, showing magnetization curves of $Co@SiO_2$ particles with core sizes of 77, 41, and 19 nm, respectively. This material is available free of charge via the Internet at http://pubs.acs.org.

References and Notes

(1) Cabuil, V. L., Bacri, J. C., Perzynski, R., Eds. Proceedings of the Sixth International Conference on Magnetic Fluids. *J. Magn. Magn. Mater.* **1993**, *122*.

(2) Aliev, F. G.; Correa-Duarte, M. A.; Mamedov, A.; Ostrander, J. W.; Giersig, M.; Liz-Marzán, L. M.; Kotov, N. A. *Adv. Mater.* **1999**, *11*, 1006.

(3) Chandrasekhar, R.; Charles, S. W.; O'Grady, K. *J. Imag. Technol.* **1987**, *3*, 55.

(4) Nakatsuka, K.; Yokoyama, H.; Shimoiizaka, J.; Funaki, T. *J. Magn. Magn. Mater.* **1987**, *65*, 359

(5) Donselaar, L. N.; Philipse, A. P. *J. Colloid Interface Sci.* **1999**, *212*, 14.

(6) Yoshizawa, A.; Nakane, Y.; Arisawa, N.; Imaizumi, H.; Sugino, K.; Harada, S. *IEEE Trans. Magn.* **1987**, *MAG-23*, 2874.

(7) De Cuyper, M.; Joniau, M. *Langmuir* **1991**, *7*, 647.

(8) Raj, K.; Moskowitz, R. *J. Magn. Magn. Mater.* **1990**, *85*, 107.

(9) Wooding, A.; Kilner, M.; Lambrick, D. *J. Colloid Interface Sci.* **1992**, *149*, 98.

(10) Massart, R. *IEEE Trans. Magn.* **1981**, *MAG-17*, 1247.

(11) Neveu, S.; Bee, A.; Robineau, M.; Talbot, D. *J. Colloid Interface Sci.* **2002**, *255*, 293.

(12) Grasset, F.; Labhsetwar, N.; Li, D.; Park, D. C.; Saito, N.; Haneda, H.; Cador, O.; Roisnel, T.; Mornet, S.; Duguet, E.; Portier, J.; Etourneau, J. *Langmuir* **2002**, *18*, 8209.

(13) Sun, S.; Zeng, H. *J. Am. Chem. Soc.* **2002**, *124*, 8204.

(14) Giersig, M.; Hilgendorff, M. *J. Phys. D: Appl. Phys.* **1999**, *32*, L111.

(15) Sun, S.; Murray, C. D.; Weller, D.; Folks, L.; Moser, A. *Science* **2000**, *287*, 1989.

(16) Rivas, J.; Sánchez, R. D.; Fondado, A.; Izco, C.; García-Bastida, A. J.; García-Otero, J.; Mira, J.; Baldomir, D.; González, A.; Lado, I.; López-Quintela, M. A.; Oseroff, S. B. *J. Appl. Phys.* **1994**, *76*, 6564.

(17) Carpenter, E. E.; Sangregorio, C.; O'Connor, C. J. *IEEE Trans. Magn.* **1999**, *35*, 3496.

(18) Park, J.-I.; Cheon, J. *J. Am. Chem. Soc.* **2001**, *123*, 5743.
(19) Sobal, N. S.; Hilgendorff, M.; Moehwald, H.; Giersig, M.; Spasova, M.; Radetic, T.; Farle, M. *Nano Lett.* **2002**, *2*, 62.
(20) Nikitenko, S. I.; Koltypin, Y.; Palchik, O.; Felner, I.; Xu, X. N.; Gedanken, A. *Angew. Chem., Int. Ed.*, **2001**, *40*, 4447.
(21) Ohmori, M.; Matijevic, E. *J. Colloid Interface Sci.* **1992**, *150*, 594.
(22) Ohmori, M.; Matijevic, E. *J. Colloid Interface Sci.* **1993**, *160*, 288.
(23) Philipse, A. P.; van Bruggen, M. P. B.; Pathmamanoharan, C. *Langmuir* **1994**, *10*, 92.
(24) Correa-Duarte, M. A.; Giersig, M.; Kotov, N. A.; Liz-Marzán, L. M. *Langmuir* **1998**, *14*, 6430.
(25) Liu, Q.; Xu, Z.; Finch, J.A.; Egerton, R. *Chem. Mater.* **1998**, *10*, 3938.
(26) Tago, Teruoki; Hatsuta, Takatoshi; Miyajima, Kanta; Kishida, Masahiro; Tashiro, Shizuka; Wakabayashi, Katsuhiko. *J. Am. Ceram. Soc.* **2002**, *85*, 2188.
(27) Lu, Y.; Yin, Y.; Mayers, B. T.; Xia, Y. *Nano Lett.* **2002**, *1*, 183.
(28) Liz-Marzán, L. M.; Giersig, M.; Mulvaney, P. *J. Chem. Soc., Chem. Commun.* **1996**, 731.
(29) Liz-Marzán, L. M.; Giersig, M.; Mulvaney, P. *Langmuir* **1996**, *12*, 4329.
(30) Ung, T.; Liz-Marzán, L. M.; Mulvaney, P. *Langmuir* **1998**, *14*, 3740.
(31) Stöber, W.; Fink, A.; Bohn, E. *J. Colloid Interface Sci.* **1968**, *26*, 62.
(32) García-Santamaría, F.; Míguez, H.; Ibisate, M.; Meseguer, F.; López, C. *Langmuir* **2002**, *18*, 1942.
(33) Henglein, A. *Ber. Bunsen-Ges. Phys. Chem.* **1982**, *86*, 301.
(34) Correa-Duarte, M. A.; Giersig, M.; Liz-Marzán, L. M. *Chem. Phys. Lett.* **1998**, *286*, 497.
(35) Giersig, M.; Ung, T.; Liz-Marzán, L. M.; Mulvaney, P. *Adv. Mater.* **1997**, *9*, 570.
(36) Iler, R. K. *The Chemistry of Silica*; John Wiley & Sons: New York, 1979.
(37) Lin, X. M.; Sorensen, C. M.; Klabunde, K. J.; Hadjipanayis, G. C. *Langmuir* **1998**, *14*, 7140.
(38) Dean, J. A., Ed., *Lange's Handbook of Chemistry*, 12th ed.; McGraw-Hill: New York, 1979.
(39) Bozorth, R. M., *Ferromagnetism*; D. van Nostrand: New York, 1951.
(40) Hochepied, J. F.; Bonville, P.; Pileni, M. P. *J. Phys. Chem. B* **2000**, *104*, 905.